Supplementary Material (ESI) for Green Chemistry
This journal is © The Royal Society of Chemistry 2011

[Supporting Information]

# One-Step and Room Temperature Synthesis of Au@Pd Core-Shell Nanoparticles with Tunable Structure Using Plant Tannin as Reductant and Stabilizer

Xin Huang, Hao Wu, Shangzhi Pu, Wenhua Zhang, Xuepin Liao,* and Bi Shi *

This journal is © The Royal Society of Chemistry 2011

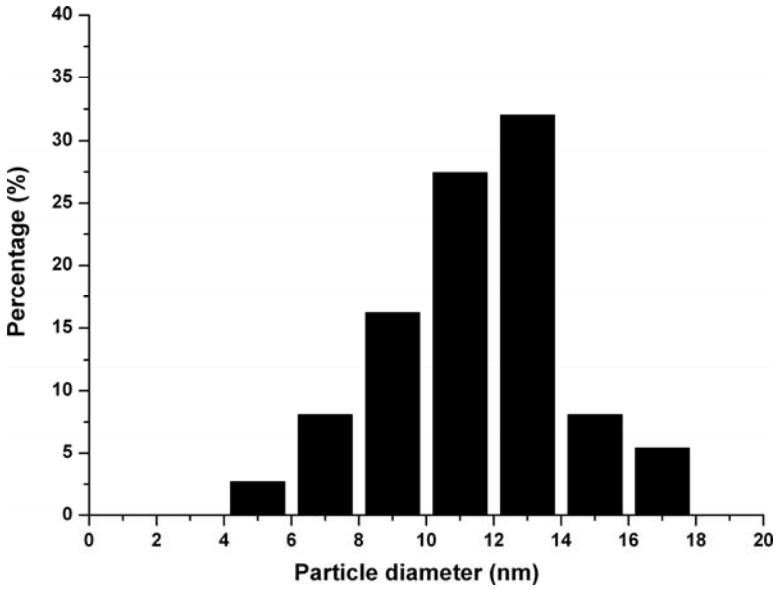


**Fig. S1**. The particle size distribution of $BT_{0.4}$-$Au_{0.5}$.

This journal is © The Royal Society of Chemistry 2011

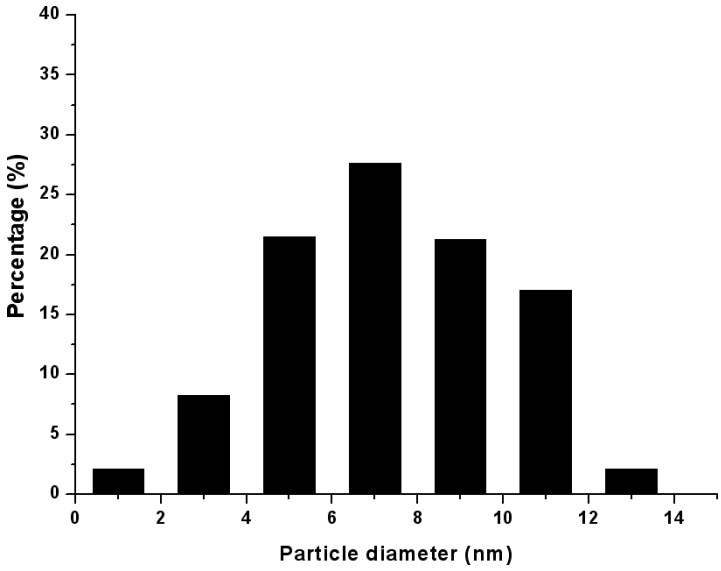


**Fig. S2**. The particle size distribution of $BT_{0.4}$-$Pd_{0.5}$.

This journal is © The Royal Society of Chemistry 2011

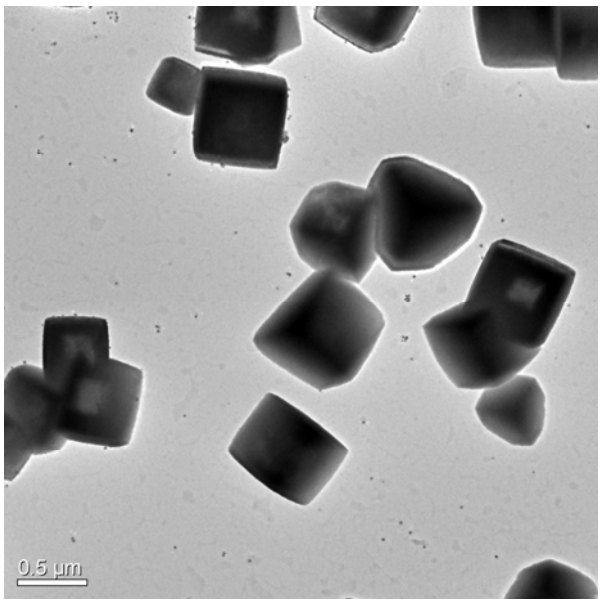


**Fig. S3**. TEM image of cubic $BT_{0.4}$-$Pd_{1.0}$.

This journal is © The Royal Society of Chemistry 2011

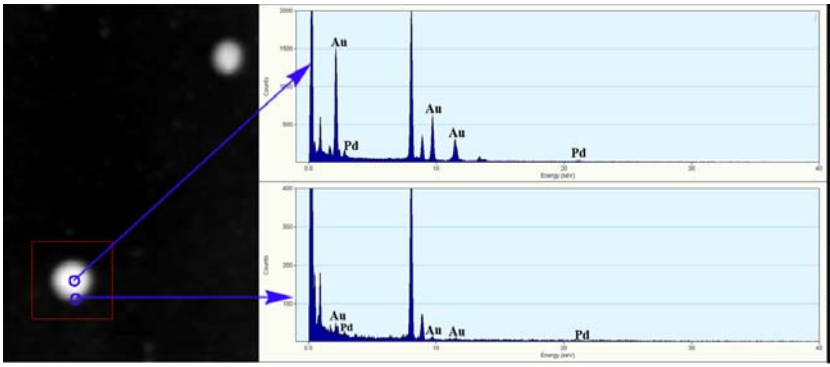


| Element | Weight % | Atomic % |
|---|---|---|
| Au | 97.29 | 94.85 |
| Pd | 2.71 | 5.15 |
| **Element** | **Weight %** | **Atomic %** |
| Au | 54.78 | 38.31 |
| Pd | 45.22 | 61.69 |

**Fig. S4**. STEM-EDS point analysis of a distinct $BT_{0.4}$-$Au_{0.5}$@$Pd_{0.01}$ NP, showing two spectra: one from the center of the particle (top), and another from the edge (bottom).

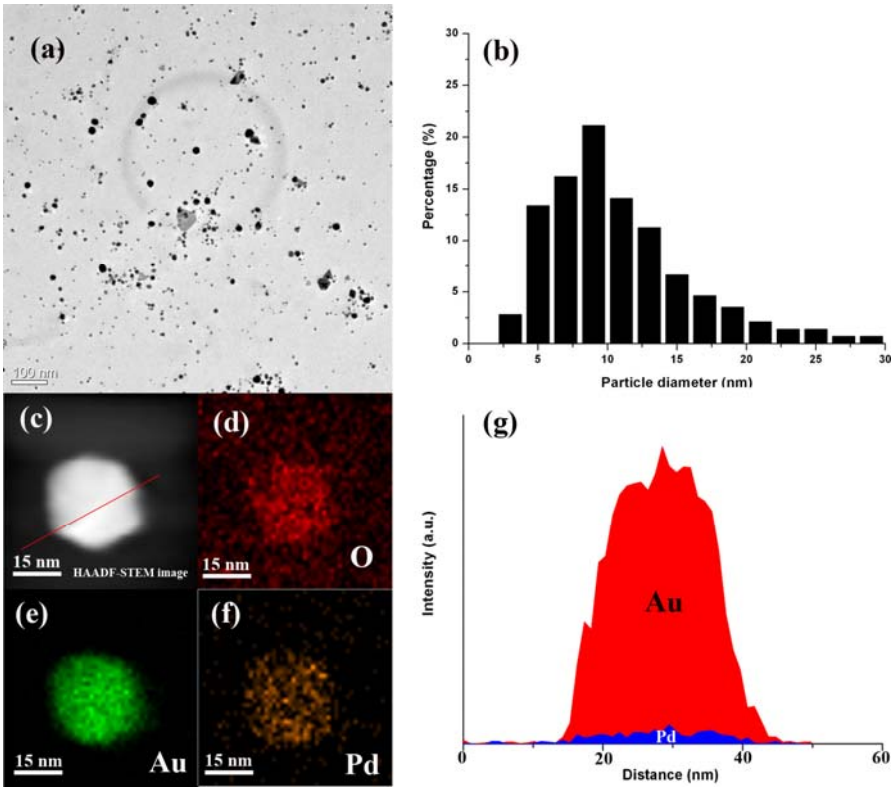


**Fig. S5**. TEM image (a) and the corresponding size distribution (b) of $BT_{0.4}$-$Au_{1.0}$@$Pd_{0.02}$. HAADF-STEM image (c) and EDS mapping images (d, e, f) of $BT_{0.4}$-$Au_{1.0}$@$Pd_{0.02}$. Cross-sectional compositional line spectra (g) of the $BT_{0.4}$-$Au_{1.0}$@$Pd_{0.02}$ in (c).

This journal is © The Royal Society of Chemistry 2011

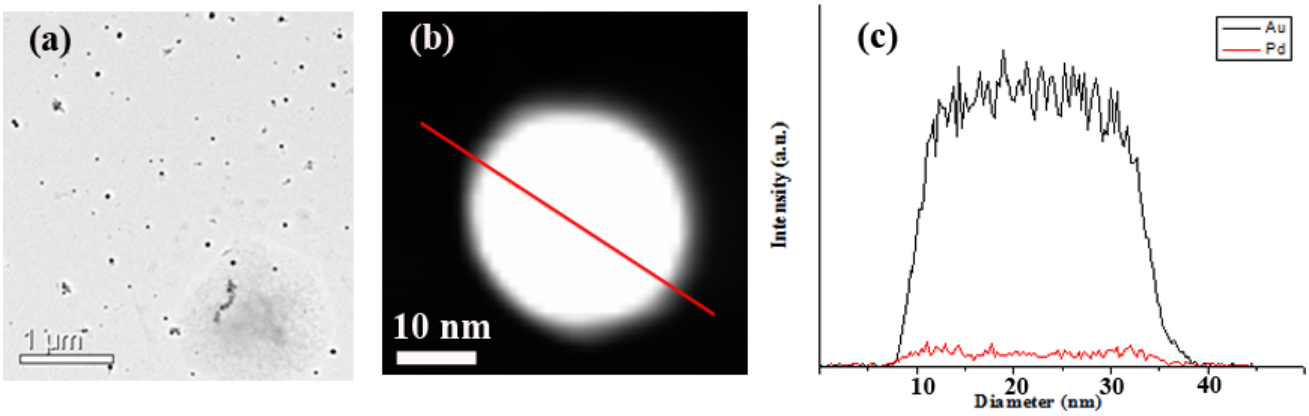


**Fig. S6**. TEM image (a), HAADF-STEM image (b), and cross-sectional compositional line spectra (c) of $BT_{0.4}$-$Au_{1.0}$@$Pd_{0.02}$ nanoparticle prepared by a step-wise reduction method.

This journal is © The Royal Society of Chemistry 2011

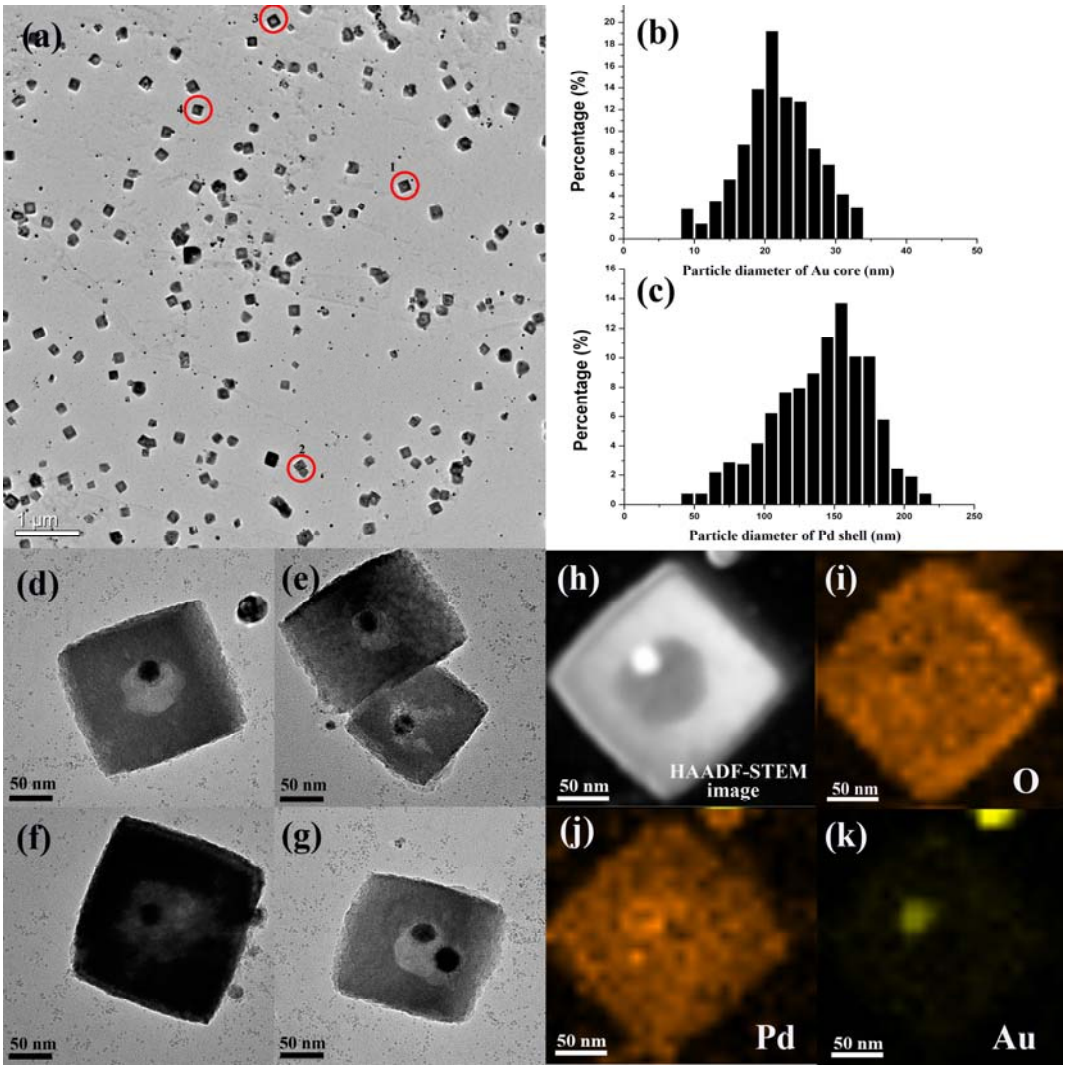


**Fig. S7**. TEM image (a) of $BT_{0.4}$-$Au_{0.5}$@$Pd_{1.0}$. The corresponding core (b) and shell size (c) distributions of cubic $BT_{0.4}$-$Au_{0.5}$@$Pd_{1.0}$. High-magnification TEM images (d, e, f and g) of cubic $BT_{0.4}$-$Au_{0.5}$@$Pd_{1.0}$ marked in (a). HAADF-STEM (h) and EDS mapping images (i, j and k) of cubic $BT_{0.4}$-$Au_{0.5}$@$Pd_{1.0}$.

This journal is © The Royal Society of Chemistry 2011

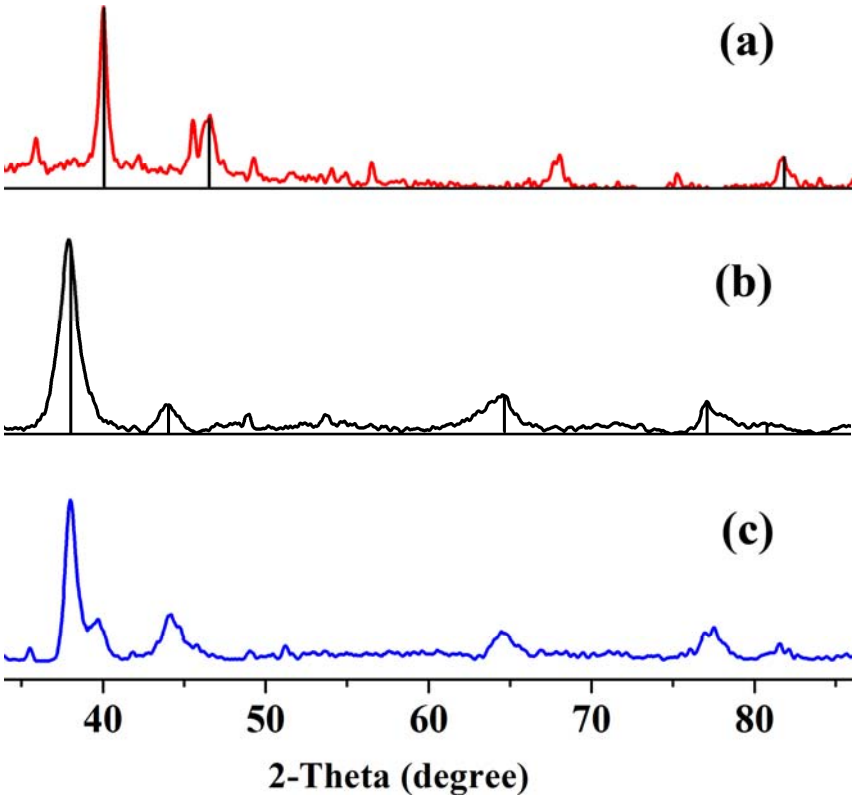


**Fig. S8**. Wide-angle X-ray diffraction patterns of $BT_{0.4}$-$Pd_{1.0}$ (a), $BT_{0.4}$-$Au_{0.5}$ (b) and $BT_{0.4}$-$Au_{0.5}$@$Pd_{1.0}$ (c).

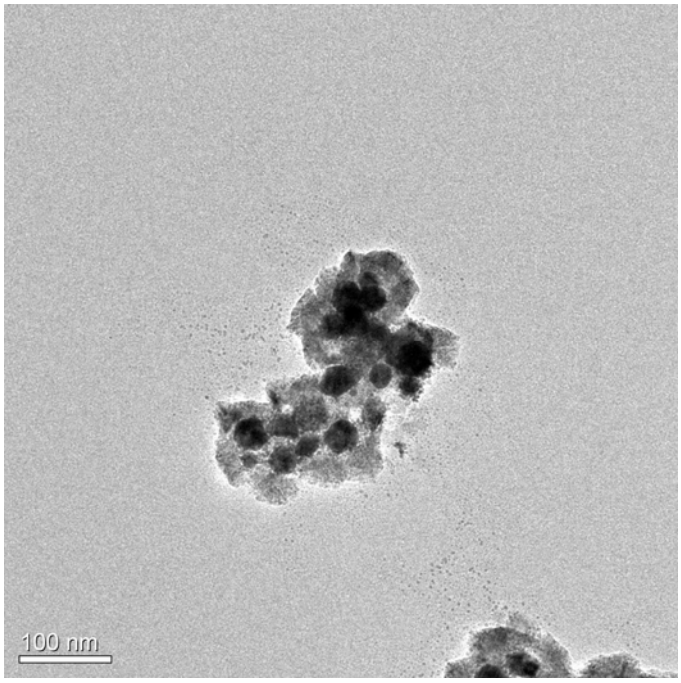


**Fig. S9**. Insufficient growth of Pd shell over Au NPs in the sample of $BT_{0.1}$-$Au_{0.5}$@$Pd_{0.5}$.

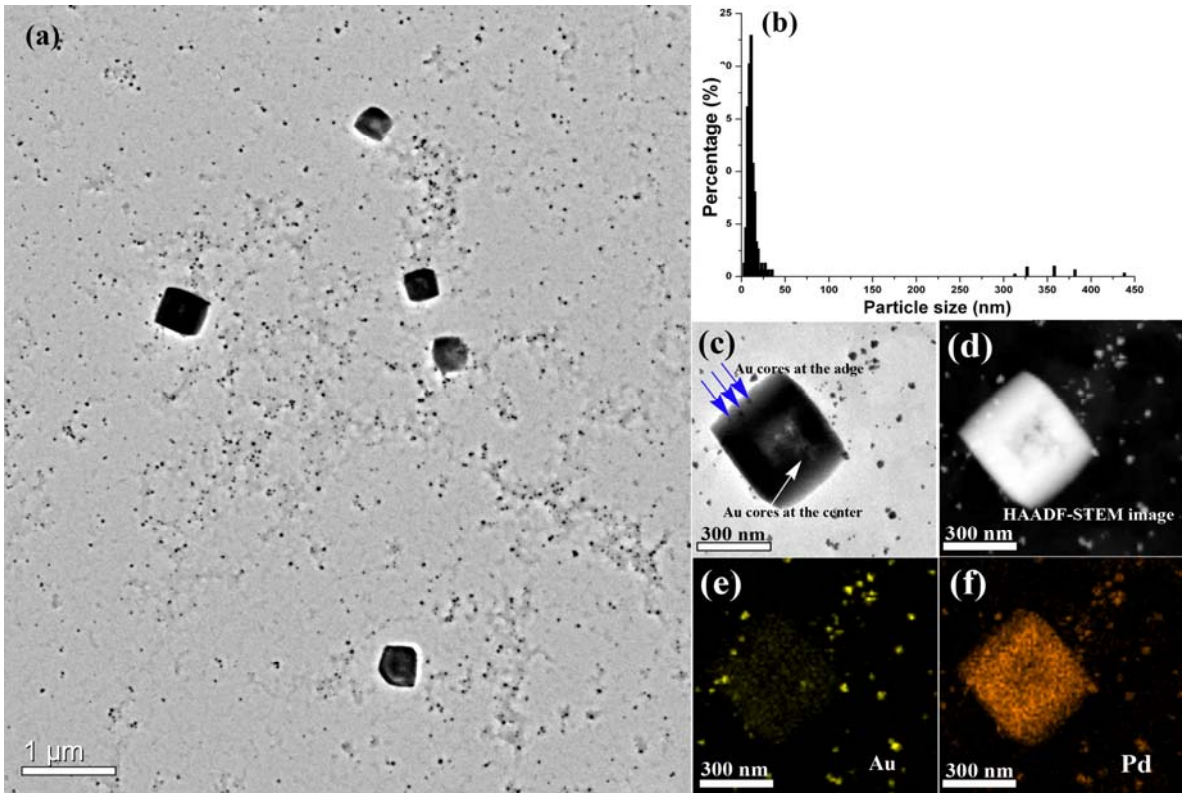


**Fig. S10**. TEM image (a) and the corresponding size distribution (b) of $BT_{0.8}$-$Au_{0.5}$@$Pd_{0.5}$. HRTEM image (c) and EDS mapping images (d, e, f) of $BT_{0.8}$-$Au_{0.5}$@$Pd_{0.5}$.

This journal is © The Royal Society of Chemistry 2011

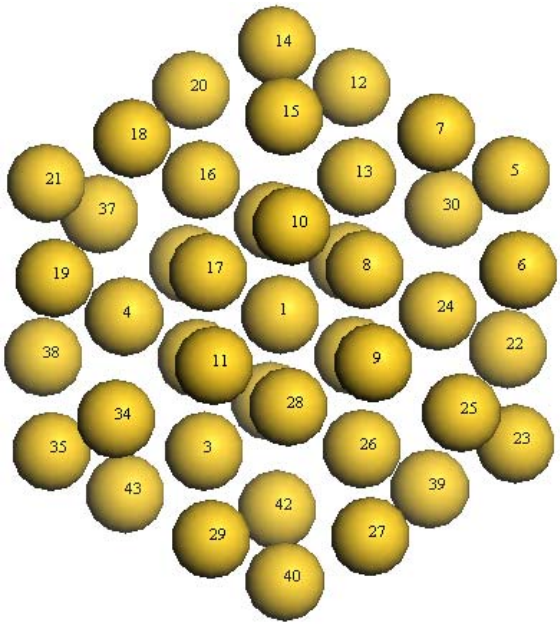


**Fig. S11**. The $Au_{43}$ cluster with numbered Au atoms.

This journal is © The Royal Society of Chemistry 2011

**Fig. S12**. The Surface charges of $Au_{43}$ cluster and Pyrogallol-$Au_{43}$ cluster.

| Numbered Au atom | Surface charge of $Au_{43}$ cluster (e) | Surface charge of Pyrogallol$_1$-$Au_{43}$ cluster | Surface charge of Pyrogallol$_2$-$Au_{43}$ cluster |
|---|---|---|---|
| Au(1) | -0.026 | -0.001 | 0.006 |
| Au(2) | 0.014 | -0.003 | 0.01 |
| Au(3) | 0.018 | -0.011 | -0.004 |
| Au(4) | 0.028 | -0.019 | 0.022 |
| Au(5) | -0.02 | 0.019 | -0.006 |
| Au(6) | -0.019 | 0.017 | -0.016 |
| Au(7) | -0.012 | 0.013 | -0.002 |
| Au(8) | 0.003 | 0 | -0.011 |
| Au(9) | -0.006 | 0.005 | -0.011 |
| Au(10) | 0.001 | -0.002 | 0.004 |
| Au(11) | 0.01 | -0.029 | 0.012 |
| Au(12) | -0.011 | 0.01 | 0.003 |
| Au(13) | 0 | 0.005 | 0.001 |
| Au(14) | -0.001 | 0.008 | -0.009 |
| Au(15) | -0.017 | -0.007 | -0.016 |
| Au(16) | 0.019 | -0.008 | 0.013 |
| Au(17) | 0.021 | -0.02 | 0.015 |
| Au(18) | 0.014 | -0.006 | -0.005 |
| Au(19) | 0.023 | -0.066 | -0.048 |
| Au(20) | 0.005 | 0.004 | 0.006 |
| Au(21) | 0.02 | -0.008 | 0.016 |

This journal is © The Royal Society of Chemistry 2011

| | | | |
|---|---|---|---|
| Au(22) | -0.019 | 0.018 | -0.015 |
| Au(23) | -0.016 | 0.018 | -0.029 |
| Au(24) | -0.008 | 0.013 | -0.022 |
| Au(25) | -0.029 | 0.006 | -0.038 |
| Au(26) | 0.001 | 0.006 | -0.033 |
| Au(27) | -0.004 | 0.007 | -0.029 |
| Au(28) | 0.012 | -0.009 | -0.017 |
| Au(29) | 0.011 | -0.041 | -0.066 |
| Au(30) | -0.035 | 0.007 | -0.01 |
| Au(31) | -0.011 | 0.011 | 0.006 |
| Au(32) | -0.003 | 0.007 | -0.009 |
| Au(33) | 0.005 | 0.001 | 0.008 |
| Au(34) | 0.004 | -0.054 | 0.005 |
| Au(35) | 0.022 | -0.028 | 0 |
| Au(36) | 0.004 | 0.007 | 0.014 |
| Au(37) | -0.003 | -0.007 | 0.013 |
| Au(38) | 0.019 | -0.003 | 0.017 |
| Au(39) | -0.011 | 0.016 | -0.021 |
| Au(40) | 0.002 | 0.003 | -0.024 |
| Au(41) | -0.003 | 0.009 | 0.003 |
| Au(42) | -0.015 | 0.003 | -0.017 |
| Au(43) | 0.012 | 0.003 | 0.008 |
| Sum | -0.001 | -0.106 | -0.276 |